Entanglement of electrons and nuclei : A most compact representation of the molecular wave function

Martin Blavier,[1,2†] Natalia Gelfand,[2†] R. D. Levine,[2,3] F. Remacle[1,2*]

[1]Theoretical Physical Chemistry, University of Liège, 4000 Liège, Belgium
[2]The Fritz Haber Research Center for Molecular Dynamics, The Hebrew University of Jerusalem, 91904 Jerusalem, Israel
[3] Department of Chemistry and Biochemistry and Department of Molecular and Medical Pharmacology, David Geffen School of Medicine, University of California, Los Angeles, CA 90095, USA

ABSTRACT

Ultrafast pumping displaces both electrons and nuclei from equilibrium so that the wave function is a double sum of separable terms for the dynamics of the electrons and nuclei. We convert the double sum into a single one by a matricization of the wave function and then generate an exact separable expression for the entangled molecular wave function. A most compact approximation with a minimum number of terms is obtained via Singular Value Decomposition. LiH and N_2 are used as an illustration: the two differ in their adiabatic electronic dynamics in the energy range accessible by a UV pulse.

*Corresponding author: fremacle@uliege.be

† Contributed equally to this work

I. Introduction

Early in the days of quantum mechanics Born and Oppenheimer demonstrated that there is a practical separation of electronic and nuclear dynamics in molecules. The high ratio of the nuclear to electronic mass is necessary for the separation. The energy gap between the ground and higher electronically excited states assists the wide applicability of the adiabatic approximation. But when the state is electronically excited, interaction with other states is the rule rather than an exception. A special case of interest in attoscience is ultrafast excitation that can coherently access several electronic states,[1-3] and so the wave function is inevitably a sum over separable components, sometimes known as the Born-Huang expansion.[4] Nowadays, this is usefully described as an entanglement[5-8] of the dynamics of the electrons and the nuclei. In extreme cases, such as high Rydberg states, one can think of an inverse separation where the slow electrons respond to the faster motion of the nuclei.[9] Recently, attention was given to a novel factorization of the wave function as a single product,[10-12] the exact factorization approach. In this approach, the total time-dependent wave function is exactly factorized as a single correlated product of a time-dependent nuclear and electronic wave function. The nuclear and electronic wave functions evolve according to coupled equations of motion involving in time-dependent potentials. This approach fully accounts for the correlation between electrons and nuclei. Another important development is a range of approximate methods based on matrix product states[13-15] suitable, in particular, for extended systems. While applied in the context of electronic-nuclear entanglement in molecules excited by attopulses, the approach proposed here is general and well suited to analyze entanglement between other kinds of molecular degrees of freedom, such as rotational and vibrational ones as is currently investigated in ultracold molecular physics.[16]

II. Matricization of the molecular time-dependent wave function

We here discuss an exact compaction of the entangled wave function. For practical purposes we show how to select the *minimal* number of separable terms for the best approximation. For conceptual purpose this compaction provides an essence of the dynamics. The key point is a systematic reduction in the number of terms in the expansion of the wave function while

keeping the best possible representation in the sense of the lowest norm of the deviation from the numerically exact result.

The approach is illustrated by two contrasting examples: the ultrafast UV pumping of LiH and of N_2 to their excited states of Σ symmetry. In the energy range accessible by a UV excitation, the two differ in their adiabatic electronic dynamics. A UV excitation brings LiH to many dissociative states that are only weakly coupled by non-adiabatic terms,[17-19] see Figure S1 of the supplementary materials, SM. The three optically UV accessible states of N_2 are bound: one is valence and two are Rydberg excited states and all three are strongly coupled by non-adiabatic terms (Figure S1 of the SM).[20-24]

The input data to our analysis are quantum dynamics computations of the wave function obtained by solving the time-dependent Schrödinger equation, as described in section S1 of the SM. The wave function is written as a double sum of separable products of a finite number electronic basis functions in an adiabatic approximation and door functions defined on a grid of equidistant points to provide a flexible description of the nuclear dynamics, equation (1):

$$\left|\Psi\right\rangle\left(t\right)=\sum_{i=1}^{N_g}\sum_{j=1}^{N_e}a_{ij}(t)\left|g_i\right\rangle\left|e_j\right\rangle \qquad (1)$$

$\left|e_j\right\rangle$ is the j'th electronic adiabatic state and $\left|g_i\right\rangle$ is a door function centered at the i'th point of the grid. N_e is the number of electronic states and N_g the number of door functions. The different electronic states as well as the different door states are orthogonal. An accurate numerical solution for the wave function, e.g.[25] for the set of time-dependent coefficients $a_{ij}(t)$, equation (S2) of the SM, is used as a basis for our development. Specifically, the matrix elements of the kinetic energy and of momentum are evaluated by a finite difference approximation, see the SM file. Typically, the non-adiabatic coupling terms of the electronic states are rapidly varying functions of the coordinate(s) so that a small grid spacing is needed and therefore the finite difference schemes converge already at a low order. The initial conditions for equation (1) is the molecule in its ground electronic state. A dipole coupling to the ultrafast laser field is included in the Hamiltonian and so treated to all orders in the strength of the field. The ultrashort laser pulse, equation (S3) of the SM, is switched early on. The time-dependent Schrödinger equation is propagated during the pulse and after its

decay because of the unfolding in time role of the nuclear-motion-induced non-adiabatic coupling between the electronic states. There is spin-orbit coupling between triplet and the three singlet states of N_2.[26] This enables a slow dissociation[24] but the time scale is longer than what we consider here.

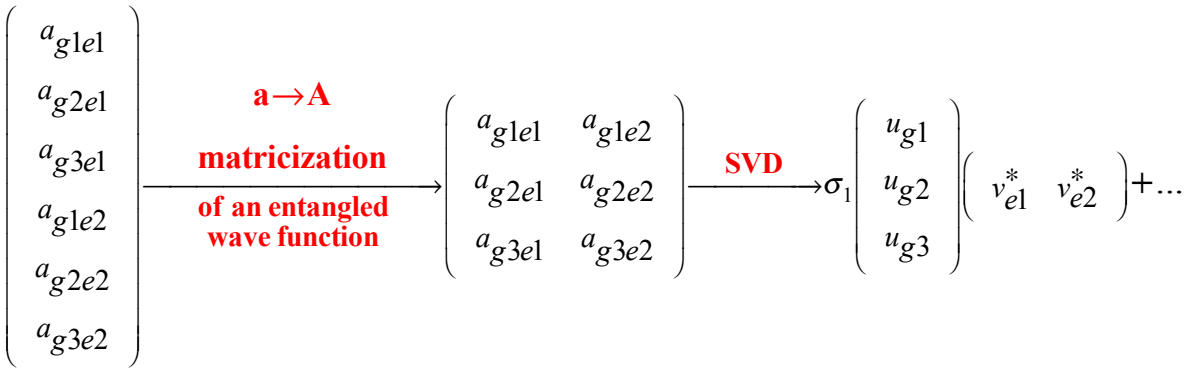

Scheme 1. Steps in the compaction of the wave function, equation (1), for three grid points and two electronic states.

The first step is to reduce the double sum of equation (1) to a single sum that is mathematically exactly equivalent. A practical way, see scheme 1, is to reshape[27] the vector of amplitude coefficients $a_{ij}(t)$ as a two-dimensional matrix **A**. It is a rectangular matrix because typically the number N_g of grid points needed for realistic accuracy is different and larger than the number N_e of electronic states. Exceptions are extended systems for which many electronic states are used to describe a band. For molecules, we take it that $N_g >> N_e$. The matrix **A**(t) has N_g rows where the elements of a given row *i* are the $a_{ij}(t)$'s for the different electronic states $j, j = 1,2,..,N_e$. Each column of **A**(t) is the amplitude of a given electronic state in the different grid locations. To convert the double sum in equation (1) to a single sum, we apply a spectral decomposition of the rectangular matrix **A**(t) using its singular values and eigenvectors,[28] see scheme 1. The singular value decomposition (SVD) theorem states that there will be at most N_e non-zero singular values σ_m labelled by the index *m*, *m*=1,...,N_e. Normalization of the wave function, equation (1),

implies that $\sum_{m=1}^{N_e} \sigma_m^2(t) = 1$. We adopt the convention that these non-negative eigenvalues are arranged in a descending order with $m = 1$ being the largest. The SVD decomposition is that at any time t any matrix element of **A**(t) can be exactly written as a sum over N_e terms

$$a_{ij}(t) = \sum_{m=1}^{N_e} \sigma_m(t) u_{im}(t) v_{jm}^{\dagger}(t) \qquad (2)$$

$\mathbf{u}_m(t)$ and $\mathbf{v}_m^{\dagger}(t)$ are the two singular eigenvectors associated with the m'th singular value $\sigma_m(t)$. $\mathbf{v}_m^{\dagger}(t)$ has N_e components and it is the m'th eigenvector of the N_e by N_e symmetric non-negative matrix $\mathbf{A}^{\dagger}(t)\mathbf{A}(t)$ with the eigenvalue $\sigma_m^2(t)$. The vector $\mathbf{u}_m(t)$ has N_g components for each value of m, $m = 1,..,N_g$, and it is the eigenvector of the larger matrix $\mathbf{A}(t)\mathbf{A}^{\dagger}(t)$. The first N_e eigenvalues are the $\sigma_m^2(t)$'s and the rest are zero. The components of the eigenvector $\mathbf{u}_m(t)$ are the grid states while the components of the eigenvector $\mathbf{v}_m(t)$ are the electronically excited states. Inserting the SVD decomposition, equation (2), in the double sum form of the wave function leads to the single sum expression over N_e separable terms

$$|\Psi\rangle(t) = \sum_{m=1}^{N_e} \sigma_m(t) |u_m\rangle |v_m\rangle \qquad (3)$$

To write equation (3), we have defined new electronic, $|v_m\rangle$, and nuclear $|u_m\rangle$ states

$$|v_m\rangle = \sum_{j=1}^{N_e} v_{jm} |e_j\rangle \quad , \quad |u_m\rangle = \sum_{i=1}^{N_g} u_{im}(t) |g_i\rangle \qquad (4)$$

$m = 1,..,N_e$ and $m = 1,..,N_g$, respectively. These states are potentially delocalized over the entire set of basis states and we wish to contrast their behavior in the two examples of LiH and N_2 and to examine what is a practical upper limit on the sum in equation (3) that we need for a good approximate representation of the wave function.

Equation (3) as written is the exact single sum over separable terms. It is the Schmidt representation[29] of N_e entangled electron-nuclear states. In any realistic problem, where the electrons and nuclei are coupled, N_e is larger than one. Yet, there are realistic cases

where for all practical aspects, including those of high spectroscopic accuracy, one separable term suffices.[30] So, our next question is "what constitutes an accurate approximation for the wave function with a smallest number of terms?" The SVD theorem[28] states that when the eigenvalues are ordered by decreasing value, as we do, truncation the sum (2) as a smaller number of terms is the best approximation in the sense of a minimal norm of the deviation. In other words, the sum (2) and therefore the expansion (3) are as accurate as possible for a given number of separable terms and this is so for each possible upper limit on the number of terms. Adding more terms in the sum can only improve the accuracy of the representation. When all N_e terms are kept, the representation is mathematically equivalent to the numerically exact wave function. A simple illustration is the equivalence of the sum $\sum_{m=1}^{N_e} \sigma_m^2(t) = 1$ and the normalization of the wave function. With fewer terms, the sum is below one. In a practical approach we keep as many terms as needed to approach unity to the desired accuracy.

III. Entanglement and compact representation of the wave function in LiH and in N_2

A UV excitation with a strong short pulse will also ionize a molecule. So for both N_2 and LiH we use a weaker pulse where the high excited states are just barely populated and a significant fraction of the population stays in the ground state. The largest singular value will not fall much below unity and the corresponding primary singular vector $|\nu_{m=1}\rangle$ will be localized on the ground electronic state. The singular values, m =1,2,3 need to be kept for the Σ states of N_2 and LiH as shown vs. time in Figure 1.

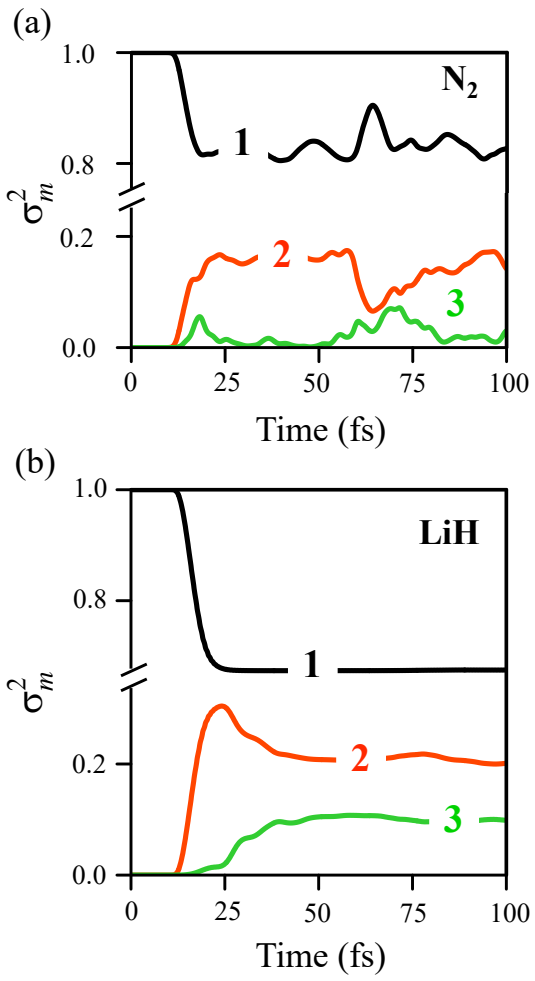

Figure 1. The larger singular values squared σ_m^2, m=1,2,3, shown as a function of time for N_2 (a) and LiH (b). The totality of excited states, $1-\sigma_1^2$, is reached just after the pulse. Beyond that time the two cases are different and an interpretation is provided in the text.

Details of the computation as well as parameters of the UV pulses are given in the SM, as well as the potential energy curves of the adiabatic states included in the computation of the dynamics for the two molecules (Figure S1). The carrier frequency and the duration of the ultrashort pulses are chosen to target a specific manifold of adiabatic electronic states. In N_2, the valence Σ_u state and the lowest Rydberg state fall within the energy bandwidth (FWHM=1.18 eV) of the pulse (Figure S1a) while in LiH, the pulse is chosen to excite the Σ_2, Σ_3.and Σ_4 states (FWHM in energy=1.84 eV), which are not bound in this energy range

(Figure S1b). In both cases, the excitation by the pulse builds a coherent superposition of states.

There are seven electronic states of LiH that are included in the expansion of the wave function. As shown in Figure 1, just three singular eigenvectors are necessary to well approximate the wave function for LiH. All the seven weights are plotted in Figure S3 of the SM and already the fourth is barely noticeable. For N_2, the reduction is moderate as four electronic states are included in the exact computation.

For N_2 (Figure 1a) the UV pulse primarily accesses the valence excited state. It has a shallower potential than the two Rydberg states, which are about as tightly bound as the ground state and are therefore localized in the Franck-Condon region, FC. The wave packet excited on the valence state moves out and then comes back to the FC region where it is strongly coupled to the lower of the two Rydberg states.[24] At that time range there is a loss of population of the valence state due to a non-adiabatic transfer to the Rydberg state. The second eigenvector $|v_2\rangle$ is primarily the valence-excited state with the lower Rydberg state contributing equally at the region of strong non-adiabatic coupling, see Figure S4 of the SM that shows the detailed composition of the singular vectors $|v_m\rangle$ on the electronic states of N_2. Note the mixing of the second and third eigenvectors as reflected in their weights, Figure 1a. It is completely analogous to the avoided crossing of the basis adiabatic states. The third eigenvector, $|v_3\rangle$, has a lower singular value, it rises at the region of strong non-adiabatic coupling where it is a linear combination of the valence excited state with the lower Rydberg state. Slightly before the rise of the third singular value the first eigenvalue is increasing as the second one is decreasing. This reflects the localization of the wave packets of the ground state and the valence state in the FC region. They can then be described by a single singular vector with $\mathbf{u_1}$ localized in the FC region (see Figure 2 below) and $\mathbf{v_1}$ having components on the two electronic states. In LiH (Figure 1b) the different adiabatic electronic states are effectively changing their population only during the fast laser pulse. Their non-adiabatic coupling is weak, see Figure S2 of the SM, so that each singular eigenvector is approximately associated with a particular electronic state, Figure S4.

The other key difference between N_2 and LiH is shown in Figure 2 where the second and the third grid eigenvector of LiH (Figure 2 d) very clearly dissociates.

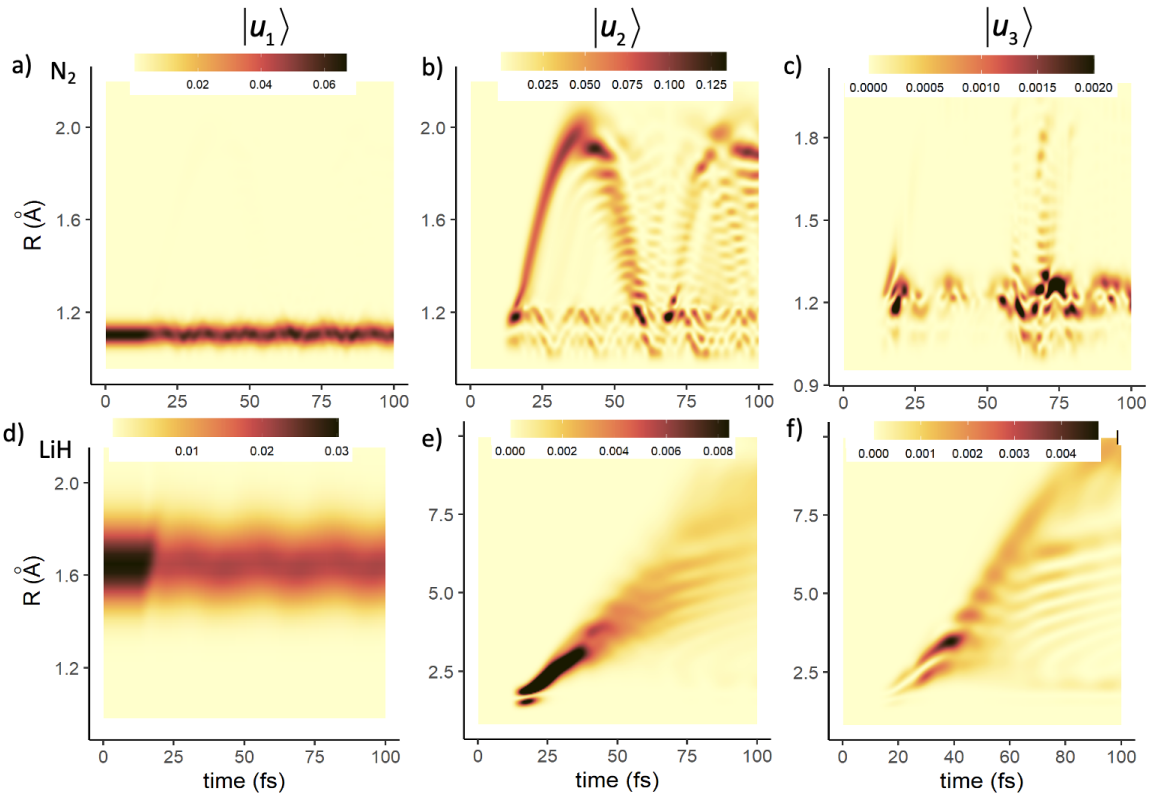

Figure 2. A heat map representation of the grid based first, second and third singular grid states in N_2 (panels a,b,c) and LiH (panels d, e, f). The distance scale is different for the two because the light H atom moves with a high amplitude. The lowest grid state $|u_1\rangle$ is essentially the ground state in both molecules. It is tightly localized in N_2 and less so in the weaker bound LiH. The states $|u_2\rangle$ and $|u_3\rangle$ differ dramatically. N_2 executes a bound motion while LiH dissociates.

The LiH potentials are quite shallow so the wave packet moves out with about a constant speed. Figure S5 of the SM shows the grid eigenvectors also for the two other isotopomers, LiD and LiT. For the heavier reduced mass the velocity is correspondingly lower. For N_2 (Figure 2) the second grid eigenvector exhibits the bound vibrational motion of the valence excited state but also shows the contribution of the Rydberg state at the time of the pulse and at the time of strong non-adiabatic coupling when the valence state returns to the FC region. The same is true for $|u_3\rangle$ which has the highest weight on the Rydberg state. The rise of the

first singular value in N_2, Figure 1, reflects the localization of the three wave packets in the FC region.

UV excitation of Σ electronic states in N_2 and LiH shows a significant entanglement of electrons and nuclei that requires three separable terms to well approximate the wave function. But the nature of the terms is quite different. In N_2 the vibrational motion remains bound and the nature of the separable terms differs very much in the region of the strong non-adiabatic coupling. The UV excited adiabatic states of LiH are dissociative and weakly coupled. A clear isotope effect of a classical mechanics origin is exhibited (Figure S5) in the grid based dissociative eigenvectors in LiX, X=H, D, T, where the heavier X atom takes longer to exit the FC region.

IV. Conclusions

Singular vectors were identified and illustrated, vectors that offer a most compact representation of the wave function when electrons and nuclei are entangled. The number of such states, needed for a good approximation, is smaller or, for LiH, significantly smaller than the number of electronically adiabatic basis states that are included in an exact numerical computation. The adiabatic components of the electronic singular eigenstates are shown in Figure S4 of the SM. For both N_2 and LiH the ultrafast pulse creates the initial entanglement and about three eigenvectors are kept, Figure 1, for a realistic approximation of the wave function. This can be stated as a Schmidt index equal 3. The time dependence of the entanglement is directly computed. The strong non-adiabatic coupling of the valence and Rydberg excited states of N_2 shows that an equally extensive entanglement evolves in time due to the coupling of adiabatic states. A very clear isotope effect is seen in the second nuclear singular state of LiH and its isotopomers, Figure S5 of the SM.

In this report we analyzed the results of the time dependent wave function computed in a full electronic basis for a single nuclear coordinate. The compaction shows that a smaller number of singular states is numerically sufficient which implies that for the future it will be computationally efficient to develop a scheme which solves directly for the time evolution of the singular states. This will be particularly so when two or more vibrational coordinates need to be used. In this case, one will have to resort to higher order SVD[31] or product matrix state decomposition.[13-15]

Author contributions

MB and NG carried out the numerical calculations. All authors have contributed equally to the analysis of the results and the writing of the manuscript.

Declaration of Competing Interest

The authors declare that they have no known competing financial interests or personal relationships that could have appeared to influence the work reported in this paper.

Acknowledgements

This work was supported by the Fonds National de la Recherche Scientifique (Belgium), F.R.S.-FNRS research grant # T.0205.20. Computational resources have been provided by the Consortium des Equipements de Calcul Intensif (CECI), funded by the F.R.S.- FNRS under Grant # 2.5020.11. Support of the COST action Attochem(CA18222) is also acknowledged. MB is supported by an Erasmus+ grant between ULiège and HUJI. NG is supported by a joint NSF-BSF project with a BSF award number 2019722.

Appendix A. Supplementary material

Supplementary data associated with this article can be found, in the online version, at https://

References

[1] M. Nisoli, P. Decleva, F. Calegari, A. Palacios, F. Martín, Attosecond Electron Dynamics in Molecules, Chem. Rev. 117 (2017) 10760-10825.
[2] M.J.J. Vrakking, F. Lepine, Attosecond molecular dynamics, Theoretical and Computational Chemistry, The Royal Society of Chemistry, Cambridge, 2019.
[3] K. Ramasesha, S.R. Leone, D.M. Neumark, Real-Time Probing of Electron Dynamics Using Attosecond Time-Resolved Spectroscopy, Ann. Rev. Phys. Chem. 67 (2016) 41-63.
[4] M. Born, K.Huang, Dynamical Theory of Crystal Lattices, Oxford University Press, Oxford, 1954.
[5] A.F. Izmaylov, I. Franco, Entanglement in the Born–Oppenheimer Approximation, J. Chem. Theory Comput. 13 (2017) 20-28.
[6] L.K. McKemmish, R.H. McKenzie, N.S. Hush, J.R. Reimers, Quantum entanglement between electronic and vibrational degrees of freedom in molecules, J. Chem. Phys. 135 (2011) 244110.

[7] J. Li, S. Kais, Entanglement classifier in chemical reactions, Sci. Adv. 5 (2019) eaax5283.
[8] M.J.J. Vrakking, Control of Attosecond Entanglement and Coherence, Phys. Rev. Lett. 126 (2021) 113203.
[9] F. Remacle, R.D. Levine, On the Inverse Born-Oppenheimer Separation for High Rydberg States of Molecules, Int. J. Quant. Chem. 67 (1998) 85-100.
[10] A. Abedi, N.T. Maitra, E.K.U. Gross, Exact Factorization of the Time-Dependent Electron-Nuclear Wave Function, Phys. Rev. Lett. 105 (2010) 123002.
[11] F. Agostini, E.K.U. Gross, Exact Factorization of the Electron-Nuclear Wave Function: Theory and Applications, in: L. Gonzalez, R. Lindh (Eds.), Quantum Chemistry and Dynamics of Excited States: Methods and Apllications, Wiley, Hoboken, 2021.
[12] F. Agostini, E.K.U. Gross, B.F.E. Curchod, Electron-nuclear entanglement in the time-dependent molecular wavefunction, Comput. Theor. Chem. 1151 (2019) 99-106.
[13] H.R. Larsson, Computing vibrational eigenstates with tree tensor network states (TTNS), J. Chem. Phys. 151 (2019) 204102.
[14] A. Baiardi, M. Reiher, Large-Scale Quantum Dynamics with Matrix Product States, J. Chem. Theory Comput. 15 (2019) 3481-3498.
[15] C. Hao, Y. Yaoliang, Z. Xinhua, X. Eric, S. Dale, Scalable and Sound Low-Rank Tensor Learning, 19th International Conference on Artificial Intelligence and Statistics, PMLR, Cadiz, 2016, pp. 1114-1123.
[16] M. Kunitski, Q. Guan, H. Maschkiwitz, J. Hahnenbruch, S. Eckart, S. Zeller, A. Kalinin, M. Schöffler, L.P.H. Schmidt, T. Jahnke, D. Blume, R. Dörner, Ultrafast manipulation of the weakly bound helium dimer, Nature Physics 17 (2021) 174-178.
[17] F.X. Gadea, Accurate ab initio calculations for LiH and its ions, LiH+ and LiH, Theor. Chem. Acc. 116 (2006) 566-575.
[18] F. Holka, P.G. Szalay, J. Fremont, M. Rey, K.A. Peterson, V.G. Tyuterev, Accurate ab initio determination of the adiabatic potential energy function and the Born–Oppenheimer breakdown corrections for the electronic ground state of LiH isotopologues, J. Chem. Phys. 134 (2011) 094306.
[19] S. van den Wildenberg, B. Mignolet, R.D. Levine, F. Remacle, Temporal and spatially resolved imaging of the correlated nuclear-electronic dynamics and of the ionized photoelectron in a coherently electronically highly excited vibrating LiH molecule, J. Chem. Phys. 151 (2019) 134310.
[20] R.S. Mulliken, W.C. Emler, Diatomic Molecules Results of Ab Initio Computations, Academic Press, New York, 1977.
[21] R.S. Mulliken, Rydberg and Valence-Shell Character as Functions of Internuclear Distance in some Excited-States of CH, NH, H2, and N2, Chem. Phys. Lett. 14 (1972) 141-144.
[22] D. Spelsberg, W. Meyer, Dipole-allowed excited states of N2: Potential energy curves, vibrational analysis, and absorption intensities, J. Chem. Phys. 115 (2001) 6438-6449.
[23] D. Stahel, M. Leoni, K. Dressler, Non-adiabatic representations of the 1-sigma-u+ and 1-pi-u states of the N2 molecule, J. Chem. Phys. 79 (1983) 2541-2558.
[24] J.S. Ajay, K.G. Komarova, F. Remacle, R.D. Levine, Time-dependent view of an isotope effect in electron-nuclear nonequilibrium dynamics with applications to N2, Proc. Natl. Acad. Sci. U.S.A 115 (2018) 5890-5895.

[25] S.A. Jayantha, K.G. Komarova, S.v.d. Wildenberg, F. Remacle, R.D. Levine, AttoPhotoChemistry: Coherent Electronic Dynamics and Nuclear Motion, in: M.J.J. Vrakking, F. Lepine (Eds.), Attosecond Molecular Dynamics, Royal Society of Chemistry, Cambridge, 2018, pp. 308-347.
[26] B.R. Lewis, S.T. Gibson, W. Zhang, H. Lefebvre-Brion, J.M. Robbe, Predissociation mechanism for the lowest Πu1 states of N2, J. Chem. Phys. 122 (2005) 144302.
[27] wikipedia, Vectorization, wikimedia foundation, https://en.wikipedia.org/wiki/Vectorization_(mathematics), 2021.
[28] G.H. Golub, C.F.V. Loan, Matrix Computations John Hopkins University Press, Baltimore, 2013.
[29] A. Ekert, P.L. Knight, Entangled quantum systems and the Schmidt decomposition, Am. J. Phys. 63 (1995) 415-423.
[30] W. Kołos, L. Wolniewicz, Nonadiabatic Theory for Diatomic Molecules and Its Application to the Hydrogen Molecule, Rev. Mod. Phys. 35 (1963) 473-483.
[31] T. Zhang, G.H. Golub, Rank-one approximation to high order tensors, Siam J. Matrix Anal. Appl. 23 (2001) 534-550.